Dynamic control of bearing-rigid formations of quadrotors

Isabelle FANTONI

ECC 2022

Workshop on Rigidity Theory applied to Dynamic Systems

July 12, 2022

Project RAPID

*Fo**R**mations of Heterogeneous **A**erial Robots for Ex**P**lorat**I**on with Variable **D**ynamics*

Financed by: Regional project, Centrale Nantes

(PhD Julian Erskine, 2018-2021)

Purpose: Improve the performance of UAV fleet with

- Dynamic formations
- Uncontrolled environments
- Heterogenous groups of agents

Scientific objectives

Robust Control

✓ Non-linear dynamics
✓ Aggressive maneuvers
? Heterogeneous capabilities

State Estimation

✓ Design localisable formations
✓ Study formation singularities
? Pose estimation by data fusion

Dynamic-sensors fusion

✗ Event-based cameras
? Heterogenous sensor fusion

Outline

Context and Modelling

Formation control objective

Model Predictive Control

Flying Parallel Robot

Modelling of UAV Bearing Formations

What is a bearing?

The unit vector from $\mathcal{A}_i$ to $\mathcal{A}_j$ expressed in $\mathfrak{F}_i$, which is a direction measurement on $\mathbb{S}^2$

$$\beta_{ij} = \mathbf{R}_i^T \frac{\mathbf{p}_{ij}}{d_{ij}} \tag{1}$$

where $\mathbf{p}_{ij} = \mathbf{p}_j - \mathbf{p}_i$ and $d_{ij} = ||\mathbf{p}_{ij}||$

Why bearing measurements

- Low cost sensor (camera)
- Onboard sensing in local frame
- Sufficient to define formation shape*

Problems

- *Unable to determine scale
- Singularities in particular configurations

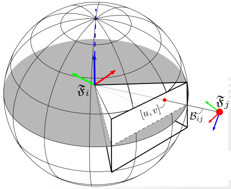

Figure 1.1: Relationship between a camera and a bearing sensor

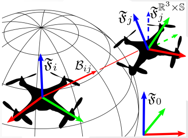

Figure 1.2: Agent $\mathcal{A}_i$ measuring the bearing β_{ij}

Formations may be modelled by a graph $\mathcal{G}(\boldsymbol{\mathcal{V}}, \boldsymbol{\mathcal{E}})$ consisting of a set of vertices $\boldsymbol{\mathcal{V}}$ and a set of edges $\boldsymbol{\mathcal{E}}$

- A vertex represents an agent
- An edge represents an exchange of information

A formation is often described using a directed (Fig. 1.3) sensing and an undirected (Fig. 1.4) communication graph.

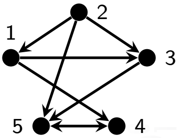

Figure 1.3: Directed graph

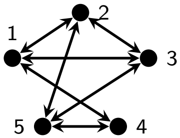

Figure 1.4: Bidirectional graph

Formation Framework

- A framework $\mathbb{F}(\mathcal{G}, \mathbf{q})$ associates a state (or embedding) $\mathbf{q_i}$ with each vertex $\mathcal{V}_i \in \boldsymbol{\mathcal{V}}$
- The embedding of $\mathcal{V}_i$ is the state $\mathbf{q}_i = [\mathbf{p}_i^T \;\; \psi_i]^T$ of $\mathcal{A}_i$ on $\mathbb{R}^3 \times \mathbb{S}^1$
- Each edge $\mathcal{E}_{ij} \in \boldsymbol{\mathcal{E}}$ corresponds to a bearing measurement β_{ij} of $\mathcal{A}_j$ wrt $\mathcal{A}_i$

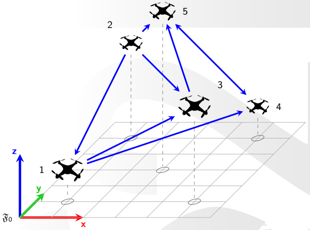

Figure 1.5: The embedding of the graph from Fig. 1.3 in $\mathbb{R}^3$

Control of UAV Formations

Primary tasks

- Agents converge to desired geometry
- Formation steers through space

Stack bearing and state vectors:

- $\mathbf{q} = [\mathbf{q}_1^T \dots \mathbf{q}_n^T]^T$ where $n = ||\mathcal{V}||$
- $\beta = [\beta_1^T \dots \beta_m^T]^T$ where $m = ||\mathcal{E}||$

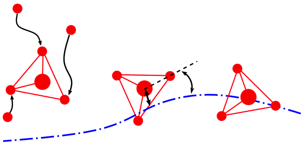

Figure 2.1: Objective of formation control

Bearing kinematic model (in $\mathfrak{F}_i$):

$$\dot{\beta} = \mathbf{B}\dot{\mathbf{q}} \tag{2}$$

Nullspace of quadrotor bearing kinematics:

$$\mathfrak{M} = \ker(\mathbf{B}) = \text{span}\left\{\mathbf{v}_{\mathcal{F}}, \dot{\psi}_{\mathcal{F}}, \dot{s}_{\mathcal{F}}\right\} \tag{3}$$

where $\mathbf{v}_{\mathcal{F}} \in \mathbb{R}^3$, $\dot{\psi}_{\mathcal{F}} \in \mathbb{S}^1$, and $\dot{s}_{\mathcal{F}} \in \mathbb{R}^1$ corresponding to a spatial translation $\mathbf{v}_{\mathcal{F}}$, a rotation $\dot{\psi}_{\mathcal{F}}$ of the formation about $\mathbf{z_0}$ and a change of scale $\dot{s}_{\mathcal{F}}$ of the formation.

Works on the rigidity controller from (Schiano et al., 2016) [1].

Why do we need better control

What is better control?

- Faster formation convergence
- More agressive steering of formation
- Fewer local minima
- More versatile constraint handling

- Known and unknown trajectories
- Adapt to difficult environments
- Maintain formation through unstable states

Solution: Model Predictive Control

A type of optimal control:

- Minimize objective function as a function of the control variable $\mathbf{u}(t)$, and the predicted output $\hat{\mathbf{x}}(t)$
- Apply current control $\mathbf{u}(0)$
- Re-run optimization with new state measurement $\mathbf{q}_0$

$$
\begin{aligned}
\min_{\mathbf{u}} \quad & \sum_{i=1}^{N_p-1} \mathcal{O}(\hat{\mathbf{x}}, \mathbf{x}^d, \mathbf{u}, \Delta t) \\
\text{s.t.} \quad & \underline{\mathbf{u}} \le \mathbf{u} \le \bar{\mathbf{u}} \\
& \mathcal{C}_{eq}(\hat{\mathbf{x}}, \mathbf{u}, \hat{\mathbf{q}}) = 0 \\
& \mathcal{C}(\hat{\mathbf{x}}, \mathbf{u}, \hat{\mathbf{q}}) \le 0
\end{aligned}
\tag{4}
$$

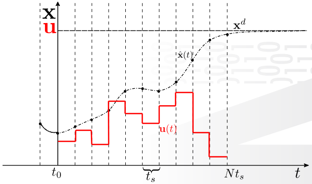

Figure 3.1: Predicted state evolution $\hat{\mathbf{x}}(t)$ for a given control $\mathbf{u}(t)$

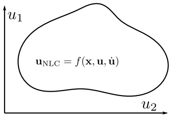

Figure 3.2: MPC Input constraints

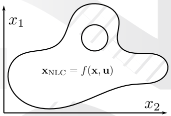

Figure 3.3: MPC state constraints

MPC objective formulation

Minimize sum of objectives

$$\mathcal{O} = \mathcal{O}_{\beta i} + \mathcal{O}_{\mathfrak{M}\ i} + \mathcal{O}_{\mathbf{u}i} \quad (5)$$

- Multi-variable optimization
- Solution lies along pareto-frontier
- Unique solution defined by weights
  - $\mathbf{Q}_{\beta} = 75$
  - $\mathbf{Q}_{\mathfrak{M}} = 25$
  - $\mathbf{Q}_{\mathbf{u}} = 5$
- High terminal gain at $k = N_p$ to reduce local minima

Bearing formation control objectives

- Minimize bearing error

$$\mathcal{O}_{\beta i} = \sum_{k=1}^{N_p} \mathbf{e}_{\beta i}^{T}(k\Delta t)\mathbf{Q}_{\beta i}\mathbf{e}_{\beta i}(k\Delta t) \quad (6)$$

- Minimize manoeuvring error

$$\mathcal{O}_{\mathfrak{M}\ i} = \sum_{k=1}^{N_p} \mathbf{e}_{\mathfrak{M}\ i}^{T}(k\Delta t)\mathbf{Q}_{\mathfrak{M}\ i}\mathbf{e}_{\mathfrak{M}\ i}(k\Delta t) \quad (7)$$

- Minimize control input

$$\mathcal{O}_{\mathbf{u}i} = \sum_{k=1}^{N_p} \mathbf{e}_{\mathbf{u}i}^{T}(k\Delta t)\mathbf{Q}_{\mathbf{u}i}\mathbf{e}_{\mathbf{u}i}(k\Delta t) \quad (8)$$

MPC Experimental results

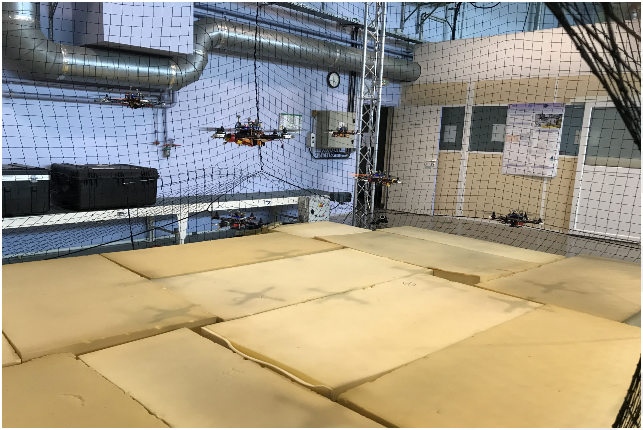

J. Erskine, R. Balderas-Hill, I. Fantoni, A. Chriette, Model Predictive for Dynamic Quadrorotor Bearing Formations, ICRA 2021

Formation control (PhD Julian Erskine, 2018-2021, RAPID)

Bearing formation controllers

- Second-order visual servoing controller
- Model predictive control
- Comparisons in constrained environments requiring dynamic maneuvering, with field of view handling, environnement collision constraints and attributes such as numerical conditioning and local minima

Study of Singularities

- Special formation configurations: is it possible to cross singularities ?
- **Generic methodology that can simplify the identification of singularities in arbitrarily large bearing formations of quadrotors**
- By respecting certain constraints in the design of formations, find a class of arbitrarily large formation graphs for which all singularities are known, and may thus be avoided, guaranteeing the rigidity of the formation

Flying parallel robot interacting with the environment

(PhD Shiyu Liu, 2019-2022)

- Background for aerial manipulation

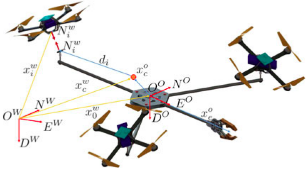

Figure 4.1: A novel robotic platform for aerial manipulation in *Nguyen et al., 2018* [11]

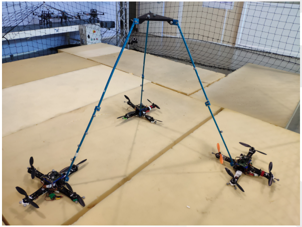

Figure 4.2: A novel flying parallel robot with three drones in *Six et al., 2018* [10]

Introduction to Flying Parallel Robot

- Analogous to parallel mechanism
- Replacing fixed actuators by UAVs

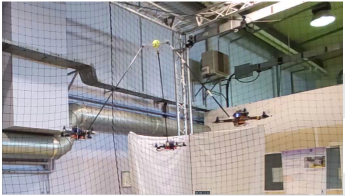

Prototype of FPR

FPR prototype is composed of:

- A moving platform
- Three rigid legs attached to the platform by means of revolute joints
- A quadrotor attached to each leg by spherical joint

Our challenge and motivation

Limitation:

- Dependence on high-rate exteroceptive measurements of robot state
  $\rightarrow$ Motion Capture (MOCAP) Systems
- Impracticality in outdoor and unmastered environments

Motivation:

- Reconstruction of robot state using only intrinsic measurements
- Control of multi-UAV parallel robots without any external localization system

Two Decentralized Controllers

- C-Controller (communicating): ζ_j are shared between the drones
- NC-Controller (non-communicating): Using of desired state ζ_j^d for the other drones on each drone i

$$\chi^d,\ \dot{\chi}^d \rightarrow \zeta_j^d = [\theta_j^d,\ \mathbf{v}_j^d] \quad \forall j \neq i$$

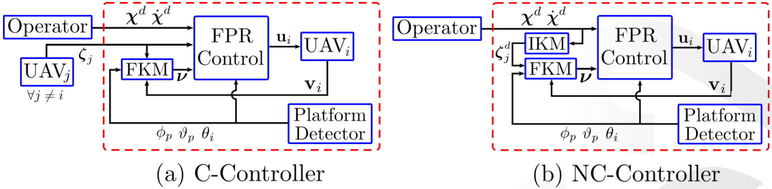

Figure 4.3: Diagram of C- and NC-Controller

Experiments on Decentralized Control

Virtual camera:

- To emulate the relative pose ${}^{p}\mathbf{T}_i$ measured by onboard camera
- Adding Gaussian noise with a standard deviation of 2cm for translations and 2° for rotations

Two experiments conducted:

- Control of internal configuration and platform orientation
- Precise positioning of the platform by teleoperation

Experiments on Decentralized Control

- Exp.1: Control of internal configuration and platform orientation

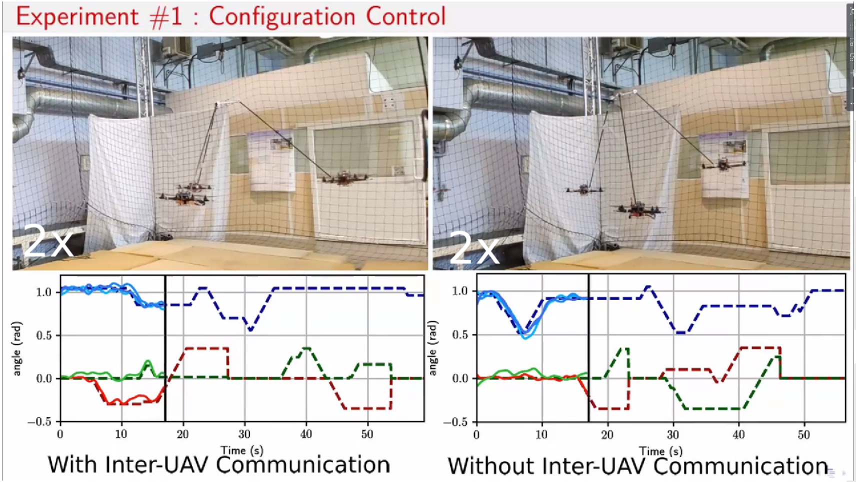

Experiments on Decentralized Control

- Exp.2: Precise positioning of the platform by teleoperation

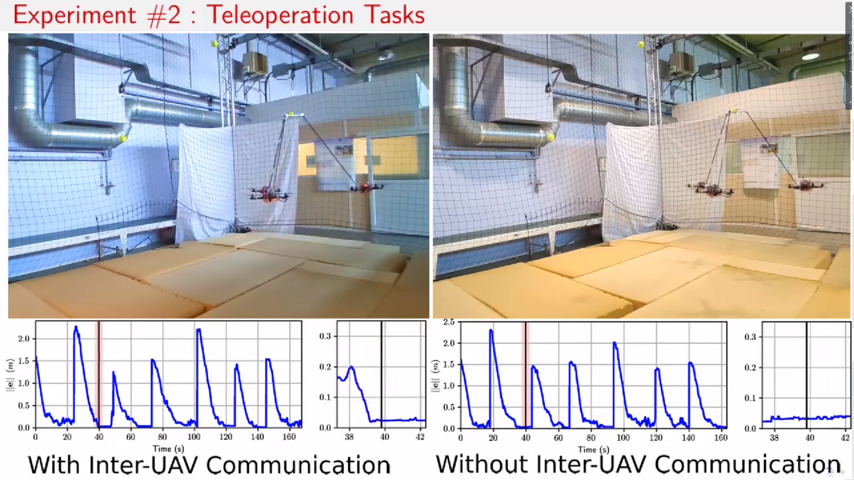

Robot-Environment Interaction

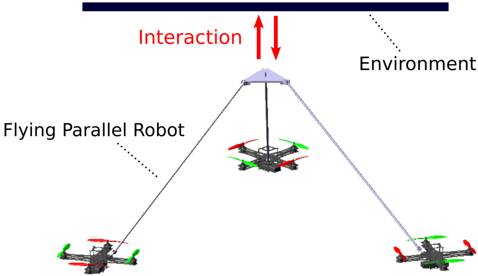

External effects:

- Modelling uncertainties
- Disturbances
- Interactions

Potential methods:

- Robust control (considering the external effects as bounded disturbances)
- Estimation of external effects (based on which a force control algorithm can be designed)

External Wrench Estimation

Dynamics of the FPR:

$$\mathbf{M}(\mathbf{q})\dot{\boldsymbol{\nu}} + \mathbf{C}(\mathbf{q}, \boldsymbol{\nu})\boldsymbol{\nu} + \mathbf{g}(\mathbf{q}) = \boldsymbol{\tau} + \boldsymbol{\tau}_e \quad (9)$$

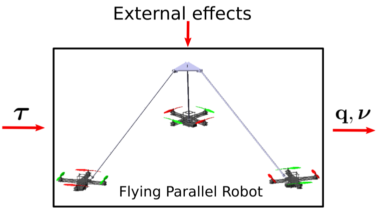

where:

- $\mathbf{q}$, $\boldsymbol{\nu}$, $\dot{\boldsymbol{\nu}}$ are the generalized position, velocity and acceleration coordinates, respectively.
- $\mathbf{M}(\mathbf{q})$, $\mathbf{C}(\mathbf{q}, \boldsymbol{\nu})$ and $\mathbf{g}(\mathbf{q})$ are the generalized inertia matrix, Coriolis matrix and gravity vector, respectively.
- $\boldsymbol{\tau}$ is the actuation wrench calculated by $\boldsymbol{\tau} = \mathbf{J}^T\mathbf{f}$

  with $\mathbf{J}$ Jacobian matrix, and $\mathbf{f} = \begin{bmatrix} \mathbf{f}_1^T & \mathbf{f}_2^T & \mathbf{f}_3^T \end{bmatrix}^T$ a vector concatenating the thrust forces of quadrotors.
- $\boldsymbol{\tau}_e$ is the external wrench.

Momentum-based Wrench Estimation

Based on the computation of generalized momentum $\mathcal{P} = \mathbf{M}(\mathbf{q})\boldsymbol{\nu}$:

$$\dot{\mathcal{P}} = \mathbf{C}(\mathbf{q}, \boldsymbol{\nu})^T \boldsymbol{\nu} - \mathbf{g}(\mathbf{q}) + \boldsymbol{\tau} + \boldsymbol{\tau}_e \tag{10}$$

$$\boldsymbol{\tau}_e = \dot{\mathcal{P}} - \mathbf{C}(\mathbf{q}, \boldsymbol{\nu})^T \boldsymbol{\nu} + \mathbf{g}(\mathbf{q}) - \boldsymbol{\tau} \tag{11}$$

Applying a first-order filtering:

$$\begin{aligned} \hat{\boldsymbol{\tau}}_e(t) =& \mathbf{K}_O \Bigg[\mathcal{P}(t) - \int_{t_0}^{t} \Bigg(\mathbf{C}\big(\mathbf{q}(t), \boldsymbol{\nu}(t)\big)^T \boldsymbol{\nu}(t) - \mathbf{g}\big(\mathbf{q}(t)\big) + \boldsymbol{\tau}(t) \\ & + \hat{\boldsymbol{\tau}}_e(t - \Delta t) \Bigg) dt - \mathcal{P}(t_0) \Bigg] \end{aligned} \tag{12}$$

where:

- $\mathbf{K}_O$ is a positive-definite diagonal matrix for estimation gain.
- $\mathcal{P}(t)$ is the momentum at current time, with $\mathcal{P}(t_0) = \mathbf{0}$.
- $\hat{\boldsymbol{\tau}}_e(t)$ is the external wrench estimate at current time.
- $\hat{\boldsymbol{\tau}}_e(t - \Delta t)$ is the previous estimate.

Impedance-based Interaction Control

A desired and virtual impedance system (mass-spring-damper system):

$$\mathbf{M}^d(\dot{\boldsymbol{\nu}}^d - \dot{\boldsymbol{\nu}}) + \mathbf{B}^d(\boldsymbol{\nu}^d - \boldsymbol{\nu}) + \mathbf{K}^d\boldsymbol{\varepsilon}_q(\mathbf{q}^d, \mathbf{q}) = \boldsymbol{\varepsilon}_\tau \tag{13}$$

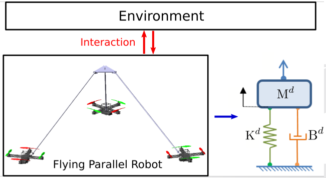

where:

- $\mathbf{M}^d$, $\mathbf{B}^d$ and $\mathbf{K}^d$ are the positive-definite diagonal matrices respectively for the desired mass, damping and stiffness of the impedance system.
- $\boldsymbol{\varepsilon}_q(\mathbf{q}^d, \mathbf{q})$ is the tracking error of the desired trajectory.
- $\boldsymbol{\varepsilon}_\tau$ is the tracking error of the desired wrench, defined as

$$\boldsymbol{\varepsilon}_\tau = -\hat{\boldsymbol{\tau}}_e - \boldsymbol{\tau}_e^d \tag{14}$$

Based on Eq.(13), an auxiliary control input can be defined:

$$\mathbf{u} = \dot{\boldsymbol{\nu}} = \dot{\boldsymbol{\nu}}^d + (\mathbf{M}^d)^{-1}\left[\mathbf{B}^d(\boldsymbol{\nu}^d - \boldsymbol{\nu}) + \mathbf{K}^d\boldsymbol{\varepsilon}_q(\mathbf{q}^d, \mathbf{q}) - \boldsymbol{\varepsilon}_\tau\right] \tag{15}$$

Impedance-based Interaction Control

By considering the dynamic model:

$$\begin{aligned}\boldsymbol{\tau} = {} & \mathbf{M}(\mathbf{q})\dot{\boldsymbol{\nu}}^d + \mathbf{M}(\mathbf{q})(\mathbf{M}^d)^{-1}\left[\mathbf{B}^d(\boldsymbol{\nu}^d - \boldsymbol{\nu}) + \mathbf{K}^d\varepsilon_q(\mathbf{q}^d, \mathbf{q}) - \varepsilon_\tau\right] \\ & + \mathbf{C}(\mathbf{q}, \boldsymbol{\nu})\boldsymbol{\nu} + \mathbf{g}(\mathbf{q}) - \hat{\boldsymbol{\tau}}_e\end{aligned} \tag{16}$$

The thrust forces of quadrotors can be finally computed:

$$\mathbf{f} = \mathbf{J}(\mathbf{q})^{-T}\boldsymbol{\tau} \tag{17}$$

From the 3-dimensional thrust forces $\mathbf{f}_i$ of each quadrotor, we can determine

- f_i^d desired thrust magnitude
- $\mathbf{h}_i^d$ desired attitude (represented by unit quaternion)

$\Rightarrow$ attitude control of quadrotors

Experimental Results

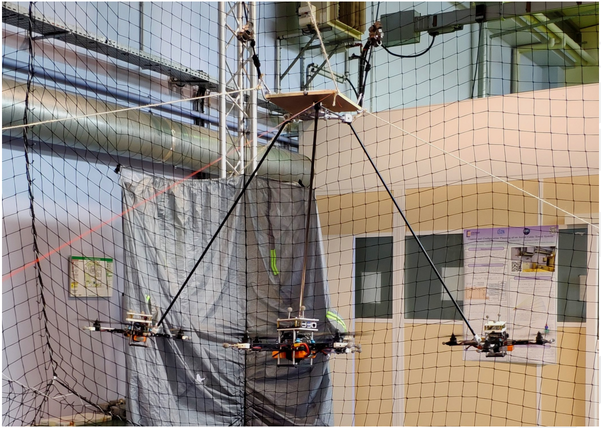

Liu, S., Fantoni, I., Chriette, A., Six, D., "Wrench Estimation and Impedance-based Control applied to a Flying Parallel Robot Interacting with the Environment," IFAC IAV 2022, July, Prague

Decentralization of FPR

Original idea:

- Use onboard measurements to reconstruct the robot state.
- Apply the control law in a decentralized way.

Onboard measurements:

- Camera (estimating relative pose)
- IMU (measuring drone's orientation)

Robot state to be reconstructed:

- Leg angles (from relative position)
- Platform orientation (from orientation information)

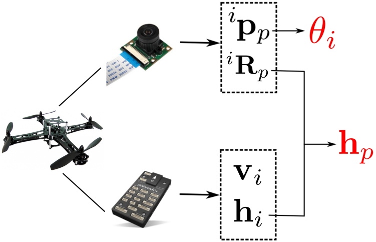

Detection of Aruco Markers (Ongoing)

- Apply the estimation and control methods in decentralized manner
- Continue to work on pose estimation by Aruco marker detection system to accomplish fully MOCAP-free version of the work

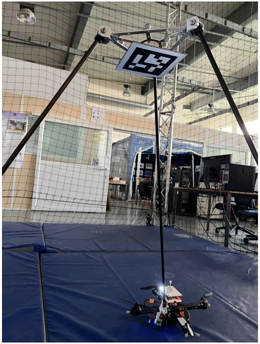

References (1)

[1] F. Schiano, A. Franchi, D. Zelazo, and P. Robuffo Giordano, "A Rigidity-Based De-centralized Bearing Formation Controller for Groups of Quadrotor UAVs", in *IEEE International Conference on Intelligent Robots and Systems*, Daejeon, South Korea, 2016, pp. 5099–5106.

[2] M. Neunert, C. De Crousaz, F. Furrer, M. Kamel, F. Farshidian, R. Siegwart, and J. Buchli, "Fast nonlinear Model Predictive Control for unified trajectory optimization and tracking", in *IEEE International Conference on Robotics and Automation*, 2016, pp. 1398–1404.

[3] M. Tognon, B. Yüksel, G. Buondonno, and A. Franchi, "Dynamic decentralized control for protocentric aerial manipulators", in *Proceedings of IEEE International Conference on Robotics and Automation (ICRA)*, 2017, pp. 6375–6380.

[4] M. Manubens, D. Devaurs, L. Ros, and J. Cortés, "Motion planning for 6-D manipulation with aerial towed-cable systems", in *Robotics: Science and Systems*, Berlin, Germany, June 24-28, 2013.

[5] M. Zhao, K. Kawasaki, X. Chen, S. Noda, K. Okada, and M. Inaba, "Whole-body aerial manipulation by transformable multirotor with two-dimensional multilinks", in *Proceedings of IEEE International Conference on Robotics and Automation (ICRA)*, 2017, pp. 5175–5182.

References (2)

[6] J. Thomas, J. Polin, K. Sreenath, and V. Kumar, "Avian-inspired grasping for quadrotor micro uavs", in *International Design Engineering Technical Conferences and Computers and Information in Engineering Conference*, Portland, Oregon, USA, August 4–7, 2013.

[7] S. Kim, S. Choi, and H. J. Kim, "Aerial manipulation using a quadrotor with a two dof robotic arm", in *IEEE/RSJ International Conference on Intelligent Robots and Systems (IROS)*, 2013, pp. 4990–4995.

[8] C. D. Bellicoso, L. R. Buonocore, V. Lippiello, and B. Siciliano, "Design, modeling and control of a 5-DoF light-weight robot arm for aerial manipulation", *2015 23rd Mediterranean Conference on Control and Automation, MED 2015 - Conference Proceedings*, pp. 853–858, 2015. DOI: 10.1109/MED.2015.7158852.

[9] P. Grau, A. Suarez, V. M. Vega, A. Rodriguez-Castaño, and A. Ollero, "Design of a high performance dual arm aerial manipulator", in *Proceedings of Iberian Robotics conference*, 2017, pp. 730–741.

[10] D. Six, S. Briot, A. Chriette, and P. Martinet, "The kinematics, dynamics and control of a flying parallel robot with three quadrotors", *IEEE Robotics and Automation Letters*, vol. 3, no. 1, pp. 559–566, 2018.

References (3)

[11] H. N. Nguyen, S. Park, J. Park, and D. Lee, "A Novel Robotic Platform for Aerial Manipulation Using Quadrotors as Rotating Thrust Generators", *IEEE Transactions on Robotics*, vol. 34, no. 2, pp. 353–369, 2018, ISSN: 15523098. DOI: 10.1109/TRO.2018.2791604.